Geotech Geol Eng (2026) 44:218
https://doi.org/10.1007/s10706-026-03729-y

ORIGINAL PAPER

Reliability Analysis of Shallow Foundations under Undrained Conditions Using Random Finite Element Limit Analysis and LRFD

Armando N. Antão · Nuno Guerra · Mário Vicente da Silva

Received: 27 February 2026 / Accepted: 8 May 2026 / Published online: 19 May 2026

Abstract This paper investigates the probability of failure of shallow foundations under centered loading and in undrained conditions, designed with the Load and Resistance Factor Design (LRFD) method. The study uses Random Finite Element Limit Analysis (RFELA), accounting for the spatial variability of undrained shear strength. A recently developed RFELA framework is employed to efficiently evaluate bearing capacity. The method combines upper bound finite element limit analysis with random field theory. It generates representative trial collapse mechanisms and maps plastic dissipation across the spatial domain, allowing for the extrapolation of collapse loads to millions of random field realizations. This strategy allows sufficiently accurate estimation of failure probabilities at small additional computational cost. Several design scenarios are systematically analyzed, considering variability of the undrained shear strength, spatial correlation lengths, load ratios, and sets of partial factors. The study examines different approaches for determining characteristic soil properties and tested two alternative methods for estimating failure probabilities. The results show that proper local soil characterization for determining characteristic values of the undrained shear strength has a relevant impact on design reliability. Furthermore, the findings indicate that standard partial factors may lead to inconsistent probabilities of failure. A new set of partial factors is proposed, providing more consistent failure probabilities across different load ratios and soil variability.

Keywords Shallow foundations · Undrained behavior · Load and resistance factor design method · Probability of failure · Soil variability · Random finite element limit analysis (RFELA)

Abbreviations

B	Footing width
$COV_{\ln s_u}$	Coefficient of variation of the logarithm of the undrained shear strength
COV_{s_u}	Coefficient of variation of the undrained shear strength
F	Total vertical load (sum of permanent and variable loads)
$F^k_{collapse}$	Collapse load corresponding to the k-th trial mechanism

Armando N. Antão, Nuno Guerra and Mário Vicente da Silva have contributed equally to this work.

A. N. Antão (✉) · M. V. da Silva
CERIS, Civil Engineering Department, NOVA School of Science and Technology, NOVA University Lisbon, 2829-516 Caparica, Portugal
e-mail: amna@fct.unl.pt

M. V. da Silva
e-mail: vicente.silva@fct.unl.pt

N. Guerra
Civil Engineering Department, NOVA School of Science and Technology, NOVA University Lisbon, 2829-516 Caparica, Portugal
e-mail: nguerra@fct.unl.pt

F_d	Design value of the action (load)
FS	Factor of safety
G	Permanent load
G_k	Characteristic value of the permanent load
k_n	Statistical coefficient (fractile of the t-distribution) for characteristic value determination
NE	Total number of finite elements in the mesh
P_f	Probability of failure
Q	Variable load
Q_k	Characteristic value of the variable load
R_d	Design value of the resistance
s_{ud}	Design value of the undrained shear strength
s_{uk}	Characteristic value of the undrained shear strength
s_u	Undrained soil shear strength
γ_G	Partial factor for permanent loads
γ_Q	Partial factor for variable loads
γ_{Rv}	Partial factor for the resistance (resistance factor approach)
γ_{s_u}	Partial factor for the undrained shear strength (material factor approach)
Γ^2	Sensitivity index
$\mathcal{D}_e^k$	Normalized plastic dissipation in element e for mechanism k
$\dot{\epsilon}^k$	Plastic strain-rate tensor for mechanism k
$\mu_{ln\, s_u}$	Mean of the logarithms of the undrained shear strength
μ_{s_u}	Mean of the undrained shear strength
$\rho_{ln\, s_u}$	Correlation function for the log-normal random field
σ_{s_u}	Standard deviation of the undrained shear strength
θ_h	Horizontal correlation length
θ_v	Vertical correlation length
Ω_e	Domain of the e-th finite element

1 Introduction

It is well known that properties of natural soils can vary spatially in a significant way. This spatial variability can therefore have an important influence on the performance of geotechnical works, whether in terms of their deformability or of their resistance, and has only begun to receive more careful attention in recent decades.

Some pioneering works on this variability or on the use of calculation tools that take this variability into account can be cited (Alonso 1976; Lump 1966; Vanmarcke 1977). However, the first works concerning geotechnical structures in which the variability of soil properties is explicitly simulated can be traced, to the authors' knowledge, to the works of Fenton and Griffiths (2001; 1996). Since then, with a consistent increase in the few last years, several authors have carried out different types of calculations that take into account the spatial variability of soil properties (Chwała 2020; Chen et al. 2022; Cheng et al. 2023a, b; Fan et al. 2024; Cheng et al. 2024; Griffiths et al. 2025; Liu et al. 2025; Fan et al. 2025).

Alonsosps16

Generally, hundreds or thousands of simulations are needed for an accurate estimation of the mean and standard deviation of the distribution of the collapse loads of a structure; in some cases (Cheng et al. 2022; Kounlavong et al. 2025), a few hundred runs were reported to suffice.

The probabilities of failure are dominated by tail events in the distributions of the safety margin (or of the safety factor). For determining probabilities of failure on the order of 10^{-2}, 10,000 samples were considered adequate (Siacara et al. 2024). For lower probabilities of failure such sample sizes are typically insufficient.

In the cases of these lower probabilities, to obtain estimates with reasonable confidence, crude Monte Carlo usually requires a very large number of simulations. For instance, when analyzing the probability of failure in cases where this should be less than 10^{-4} (EN 1997–1 2004), failure is so rare that it is unlikely to be observed in a small sample size, making accurate estimation difficult without substantially increasing the number of runs (or using variance-reduction techniques). For this purpose Li et al. (Li et al. 2025) used 10^6 realizations (in some cases 10^7) to support their conclusions on slope stability.

Therefore, the probability of failure is often estimated by fitting distributions to the data resulting from the calculations performed, as in Simões et al. (Simões et al. 2020). In their procedure, a statistical distribution is fitted to the available data and the probability of failure is then obtained by using the tail values given by this distribution. Unfortunately, this fitting, despite ensuring a good approximation of the existing data, translates into an extrapolation in the tail zone that may induce significant errors in the estimated probability of failure.

The aim of the present work is to achieve a good representation of those tails for a design case of a continuous footing supported by a soil responding under undrained conditions. This is obtained by performing a massive number of collapse calculations using a methodology recently presented by Vicente da Silva and Antão (Da Silva and Antão 2025b), in which the estimation of the collapse loads is performed with modest computational cost, allowing for the execution of several millions of calculations.

2 Problem Definition and Methodology

2.1 The Problem

The geometry and loading of the case study are illustrated in Fig. 1. The case study deals with a continuous footing of width B equal to 3 m, supported by a soil that, when subjected to loading, is considered to respond under undrained conditions. The force F is vertical, centered and is due to a permanent load, G, and to a variable load, Q.

The undrained soil shear strength is modeled by Tresca's criterion, and the value of this shear strength, s_u, varying spatially, has a lognormal distribution with mean μ_{s_u} and standard deviation σ_{s_u}.

The correlation function of the undrained shear strength at two points A and B is of the Markov type:

$$\rho_{\ln s_u}(A,B) = \exp\left[-2\sqrt{\left(\frac{\|AB\|_h}{\theta_{\ln s_u,h}}\right)^2 + \left(\frac{\|AB\|_v}{\theta_{\ln s_u,v}}\right)^2}\right] \tag{1}$$

where $\|AB\|_h$ is the horizontal distance between the two points A and B, $\|AB\|_v$ is the vertical distance

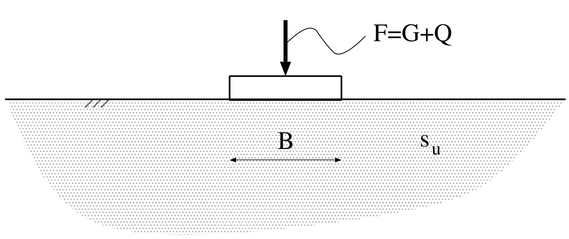

Fig. 1 Geometrical and loading conditions

between the same points, $\theta_{\ln s_u,h}$ and $\theta_{\ln s_u,v}$ are the horizontal and vertical correlation lengths of the associated variable $\ln s_u$. It should be noted that although $\theta_{\ln s_u}$ and θ_{s_u} differ, they are quite similar (Puła and Griffiths 2021). In the following, the symbols θ_h and θ_v will be used instead of $\theta_{\ln s_u,h}$ and $\theta_{\ln s_u,v}$, respectively.

Assuming a set of values of μ_{s_u}, σ_{s_u}, θ_h and θ_v, the spatial distribution of the undrained shear strength is determined by assigning a value of s_u to each cell in an orthogonal grid that spatially covers the soil zone whose strength properties are to be modeled. In the present work, two alternative methods are employed in this process: a Cholesky-based method enhanced with the Latin Hypercube Sampling (LHS), used according to a description by Olsson et al. (2003) and the method of Local Average Subdivision (LAS), based on the numerical implementation provided by Fenton (2025), following the work by Fenton and Griffiths (Fenton and Griffiths 2008).

The procedure described allows a certain number of realizations (or samples) to be obtained. The domain of the samples measures 6B horizontally by 3B vertically. It is discretized in statistical squared elements of $0.2 \times 0.2\,\mathrm{m}^2$, resulting in a 90×45 orthogonal grid. This constitutes the statistical mesh. A previous study (Simões et al. 2020) showed that, for the isotropic case, results obtained for mesh size equal to $B/10$ were practically equal to the ones obtained for $B/20$, for the correlation lengths being considered. In the present study a conservative value of $B/15$ was adopted. Also, for another type of problem (compressive strength), other authors (Huang and Griffiths 2015) reached similar conclusions.

Figure 2 shows two realizations obtained with the LHS method, for $\mu_{s_u} = 100\,\mathrm{kPa}$, coefficient of variation $COV_{s_u} = \sigma_{s_u}/\mu_{s_u} = 0.50$, $\theta_v = 1\,\mathrm{m}$ and $\theta_h = 45\,\mathrm{m}$. This mean value was used throughout the present paper; the results, however, are not dependent on this value. Following Phoon and Kulhawy (Phoon and Kulhawy 1999), calculations were made using two values of θ_v: 1 and 6 m, corresponding to a low and to a high value of this parameter, and the value of $\theta_h = 45\,\mathrm{m}$ was considered in all calculations, as it corresponds to the lower range of this parameter, which is expected to have the largest influence on the results. For each sample, a collapse load is obtained.

We highlight as relevant differences between the two methods of sample generation that LHS, while

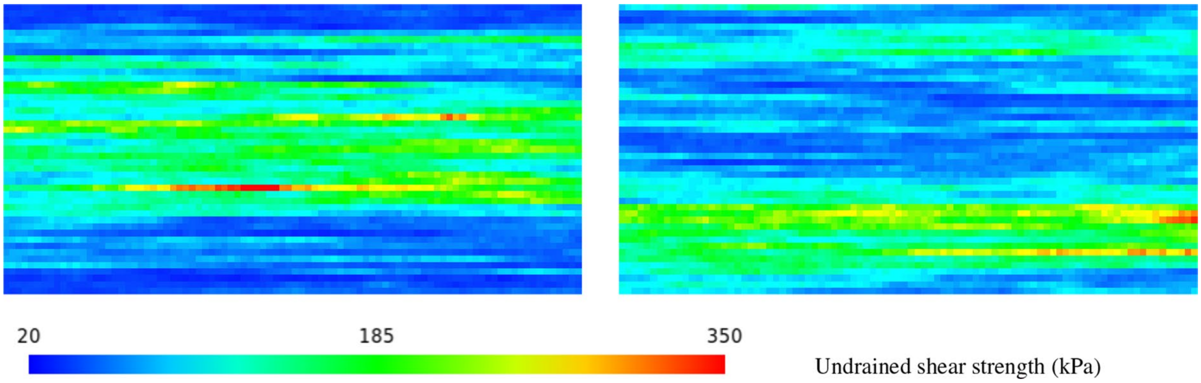

Fig. 2 Examples of two realizations of the undrained shear strength distribution, using LHS

computationally more intensive, generates greater sample diversity, reducing the number of simulations needed for a representative statistical coverage, whereas LAS focuses solely on reproducing spatial correlations in the soil properties.

The key question we aim to answer is whether when applying a load defined by a safety code such as the Eurocode 7 (EC7) (EN 1997–1 2004), the safety margins are in accordance with what is defined by this code. The methodology used to answer this question is presented in the following subsections.

2.2 Design Values

In this work the Load and Resistance Factor Design method is used. The safety of a footing against vertical bearing failure of the soil is verified if:

$$F_d \leq R_d \tag{2}$$

where F_d and R_d are the design values of the action and of the resistance, respectively, obtained by applying appropriate partial factors.

These partial factors are applied to actions, to material properties and/or to resistances. Considering a permanent and a variable load, both vertical, with characteristic values G_k and Q_k, the design value of the action is:

$$F_d = \gamma_G G_k + \gamma_Q Q_k \tag{3}$$

where γ_G and γ_Q are the partial factors for permanent and variable loads, respectively.

The bearing capacity for the case represented in Fig. 1, where no embedment of the footing is considered, and the loading is vertical and centered, can be determined using the exact solution given by:

$$q_r = (2 + \pi) s_u \tag{4}$$

A characteristic value of this bearing capacity can be determined if a characteristic value of s_u, s_{uk}, is used in the previous equation. The design value of the resistance, R_d, can be determined using the Material Factor Approach (MFA), where a partial factor γ_{s_u} is applied to s_{uk}:

$$s_{ud} = s_{uk} / \gamma_{s_u} \tag{5}$$

and therefore R_d becomes:

$$R_d = B(2 + \pi) \frac{s_{uk}}{\gamma_{s_u}} \tag{6}$$

Alternatively, R_d can be determined using the Resistance Factor Approach (RFA), where a partial factor γ_{Rv} is applied to the resistance:

$$R_d = \left(B(2 + \pi) s_{uk} \right) \frac{1}{\gamma_{Rv}} \tag{7}$$

Equations (6) and (7) show that for the simplified problem being analyzed, the partial factors γ_{s_u} and γ_{Rv} affect R_d in the same way. Therefore, only the formulation of Eq. (6) will be considered in this work.

2.3 Characteristic Values of the Strength Parameter

As the Lognormal distribution is considered for s_u, the characteristic values of the strength parameter, s_{uk}, are determined using the following equation (Orr et al. 2025):

$$s_{uk} = \exp\left[\mu_{\ln s_u}\left(1 - k_n COV_{\ln s_u}\right)\right] \tag{8}$$

where $\mu_{\ln s_u}$ is the average of the logarithms of s_u, $COV_{\ln s_u}$ is the coefficient of variation of $\ln s_u$, and k_n is a coefficient that depends on the number of values used to calculate $\mu_{\ln s_u}$ and on the level of the knowledge of $COV_{\ln s_u}$.

Two main situations are studied. In the first one, a single value of s_{uk} is used for all samples and is obtained from the values of μ_{s_u} and COV_{s_u} used for generating the samples. In the second one, a different value of s_{uk}, obtained from simulating soil characterization, is used for each sample.

2.3.1 *Situation 1: Single Value of s_{uk}*

In this situation, the values of both μ_{s_u} and COV_{s_u} are taken equal to the ones used for generating the samples (μ_{s_u} and COV_{s_u} are input parameters for generating the samples; $\mu_{\ln s_u}$ and $COV_{\ln s_u}$ are determined from these (Fenton and Griffiths 2008). For this situation, k_n is determined considering previous knowledge of the coefficient of variation, and is taken equal to Orr et al. (2025):

$$k_n = N_{95}\sqrt{\Gamma^2 + \frac{1}{n}} \tag{9}$$

where N_{95} is the 95% quantile of the standard normal distribution, equal to 1.645, n is set equal to 30 (NP122 2010) and Γ^2 is a sensitivity index. This index accounts for the sensitivity of the limit state to the spatial variability of the soil (Vanmarcke 1980):

$$\Gamma^2 = \frac{\theta}{L} \tag{10}$$

where θ is the scale of fluctuation and L is the extent of the volume of the soil involved in the limit state. Three different values of Γ^2 are considered:

- $\Gamma^2 = 0$, which assumes that L is very large when compared to θ and that therefore the limit state is quite insensitive to the soil spatial variability, meaning that the characteristic value is taken as an estimate of the mean value;
- $\Gamma^2 = 1$, which assumes that θ and L are of similar magnitudes, meaning that the limit state is very sensitive to the soil spatial variability and therefore the characteristic value corresponds to the 5% (or 95%) fractile values;
- Γ^2 is an intermediate value, where, in the case under analysis, the relevant value of θ is θ_v and L is assumed equal to $0.7B$, which is the approximate depth of the theoretical mechanism for homogeneous soil. For the case study under analysis, when θ_v is 1 m, Γ^2 is equal to $1\,\text{m}/(0.7 \times 3\,\text{m}) = 0.48$; when θ_v is 6 m, Γ^2 given by Eq. (10) would lead to a value greater than 1, and therefore the limit state is considered very sensitive to the soil spatial variability and a value of Γ^2 equal to 1 is assumed.

For this first situation, where, as described, the values of μ_{s_u} and COV_{s_u} are taken equal to the ones used for generating the samples, for each value of Γ^2 considered, a single value of s_{uk} is assumed for all samples. For the mean value of s_u considered in the present work (100 kPa) the characteristic values s_{uk} are presented in Table 1 for the different values of COV_{s_u} and Γ^2 used.

2.3.2 *Situation 2: s_{uk} Determined from Simulating Soil Characterization, in Each Sample*

In this second situation, soil characterization is simulated for each sample, assuming the values of the undrained shear strength in a vertical line below the center of the footing, down to a depth $D = B$.

Table 1 Values of s_{uk} (kPa) for $\mu_{s_u} = 100$ kPa obtained for the first situation studied

COV_{s_u}	0.1	0.2	0.3	0.4	0.5
$\Gamma^2 = 0$	96.57	92.40	87.70	82.70	77.61
$\Gamma^2 = 1$	84.22	70.42	58.63	48.75	40.60
$\Gamma^2 = 0.48$	88.47	77.65	67.77	58.96	51.26

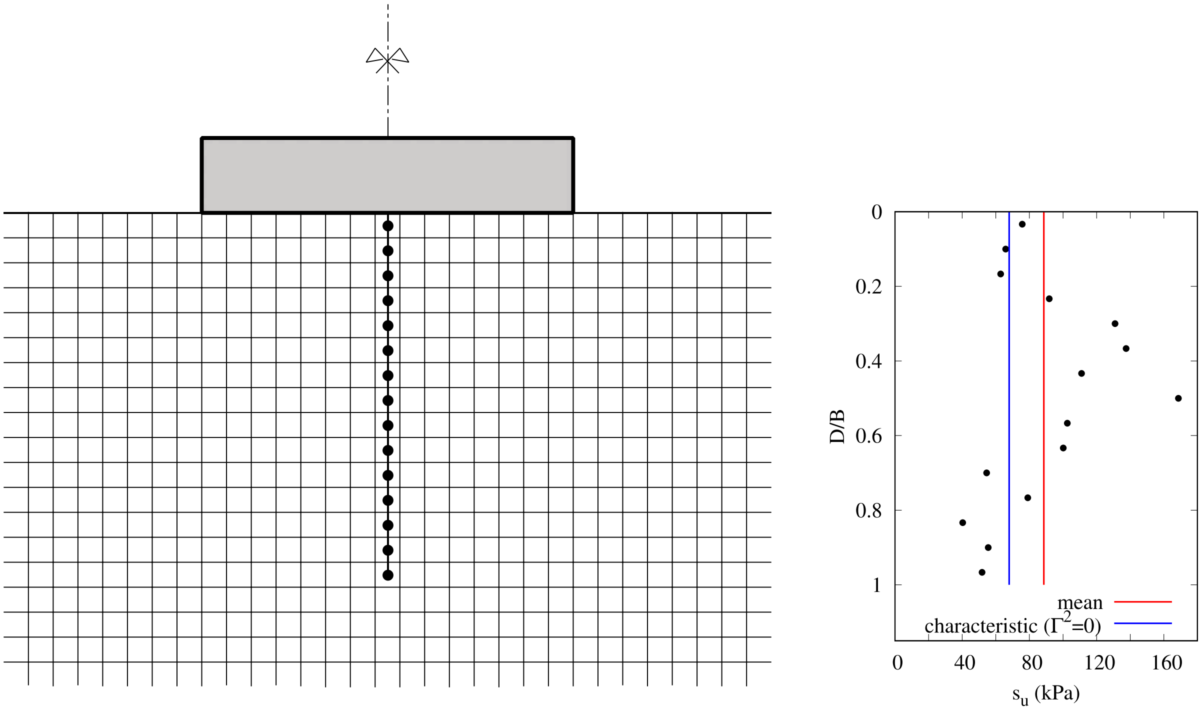

Fig. 3 Simulation of characterization

Figure 3 shows the zone of the statistical mesh underneath the foundation and the collection points for the undrained shear strength values; for this situation the number of points, n, is equal to 15. It should be noted that the values are directly taken from the random field realizations, with no simulation of characterization errors considered. The figure shows an example for $COV_{s_u} = 0.5$ and $\theta_v = 1$ m.

For each sample the average of the undrained shear strength and the coefficient of variation are determined from the values taken from the simulation of soil characterization, and Eq. (8) is applied, resulting in different values of s_{uk}. For this situation, k_n is determined assuming no prior knowledge of the coefficient of variation and it is determined using:

$$k_n = t_{95}^{n-1}\sqrt{\Gamma^2 + \frac{1}{n}} \tag{11}$$

where t_{95}^{n-1} is Student's t-factor, evaluated for a 95% confidence level and $n-1$ degrees of freedom, and n is the number of values of the undrained shear strength taken from each simulation of characterization. The same three values of the sensitivity index shown in Table 1 are also considered in the second situation.

The graphic in Fig. 3 includes the values of the average of the undrained shear strength and the characteristic value considering $\Gamma^2 = 0$.

2.4 Design Values of the Action and of the Resistance

The inequality (2) defines which set of actions is applicable to ensure safety. In this work it will be assumed that design is performed considering the equality in the above mentioned inequality. In this case, having determined the characteristic value of the strength property and considering that the variable load can be written as a factor of the permanent load ($Q = XG$, with $X \geq 0$)), from Eqs (3) and (6) the maximum value of permanent load that would ensure safety when using MFA would be:

$$G_{MFA}^{\max} = \frac{B\,(2+\pi)\frac{s_{uk}}{\gamma_{s_u}}}{\left(\gamma_G + \gamma_Q X\right)} \tag{12}$$

2.5 Random Finite Element Method

The force given by Eq. (12) represents the maximum permanent load that satisfies the safety criterion. To determine the "real" bearing capacity of each sample, a recently developed random finite element limit analysis (RFELA) method, proposed by Vicente da Silva and Antão (Da Silva and Antão 2025b), is applied. The method consists of a three-step procedure, the first of which involves generating a representative set of trial collapse mechanisms.

These mechanisms are obtained using a strict upper bound finite element limit analysis (FELA) tool (Vicente da Silva et al. 2020), which enables the determination of collapse loads and corresponding failure mechanisms for various geometries and both isotropic and anisotropic criteria, specifically under undrained loading conditions, and shows a good agreement with lower-bound calculations (Santana et al. 2018; Viana et al. 2019; Antão et al. 2019, 2021; Da Silva and Antão 2025a).

This exclusive FELA-based approach is based on triangular meshes with quadratic approximations for the velocity field (Antão et al. 2012) and has previously been applied to media with property distributions similar to those considered in the present work (Simões et al. 2014, 2020; Rogério et al. 2024). However, a drawback of relying solely on FELA, as in our earlier applications, is the computational time required to determine collapse loads. Although it is a highly effective analysis method, it does not allow more than a few hundred thousand calculations to be performed within a reasonable time frame.

Therefore, within the current framework, a diverse and representative set of random field realizations is generated using the LHS method to ensure adequate diversity. In the present case, 4051 LHS samples are generated, and the corresponding collapse loads and failure mechanisms are determined through FELA, which serve as the trial collapse mechanisms. The number of samples represents the minimum required by the LHS methodology for the statistical mesh, equal to the number of statistical elements plus one ($90 \times 45 + 1 = 4051$ in the present study). By adopting this approach, the number of FELA computations and consequently the associated computational effort is substantially reduced.

We note that, where when the RFELA framework was first introduced (Da Silva and Antão 2025b), the same footing problem was analyzed in terms of the accuracy of the collapse load estimation. That study showed that the adopted number of 4051 mechanisms leads to highly accurate collapse load estimates, with relative errors below 1% when compared with a full upper-bound FELA analysis using a similar finite element mesh. This provides supporting evidence that the chosen set of trial mechanisms is sufficient for the level of accuracy required in the present work.

In the second step of the procedure, the plastic dissipation associated with the failure mechanisms is mapped into the cells of the 90×45 orthogonal grid used to generate the spatial distribution of soil properties. Additionally, as part of this step, the plastic dissipation in each cell is normalized by the respective undrained shear strength.

In the third and final step, the mapped and normalized plastic dissipations associated with each trial mechanism are used to extrapolate, accurately and efficiently, the upper bound collapse loads for any other sample with the same statistical properties as the initial LHS samples, namely, the same mean, standard deviation, and correlation lengths.

In practical terms, for each trial mechanism k, obtained from a full FELA analysis, the collapse load F^k_{collapse} of a footing resting on weightless soil governed by the Tresca criterion can be expressed in terms of the total plastic dissipation as (Vicente da Silva et al. 2020):

$$F^k_{\text{collapse}} = \sum_{e=1}^{NE} s^k_{u,e} \mathcal{D}^k_e \tag{13}$$

with

$$\mathcal{D}^k_e = \int_{\Omega_e} \mathrm{tr}(|\dot{\varepsilon}^k|)\, d\Omega \tag{14}$$

where NE denotes the total number of finite elements, $s^k_{u,e}$ is the undrained shear strength associated with the e-th finite element, and Ω_e is its corresponding domain. Furthermore, $\mathcal{D}^k_e$ represents the normalized plastic dissipation, where $\mathrm{tr}(|\dot{\varepsilon}^k|)$ denotes the sum of the absolute values of the principal strain-rate components associated with the velocity field of the k-th collapse mechanism.

Note that this velocity field is isochoric to satisfy the normality flow rule and is scaled such that the external forces produce a unit work rate, which is standard practice in FELA optimization. Consequently, the collapse load can be estimated for any other spatial distribution of undrained shear strength by replacing in (13) the term $s_{u,e}^k$ with the new shear strength values $s_{u,e}^{\text{new}}$. The accuracy of this estimate depends on how different the new shear strength field is compared to the original one, especially in the regions of higher plastic dissipation. This procedure enables the efficient evaluation of collapse loads for a large number of realizations without additional FELA computations. Further details on the RFELA formulation and implementation of this approach can be found in Vicente da Silva and Antão (2025b).

In the present work, this extrapolation was performed for 1, 10, or 100 million samples, depending on the case under analysis. To provide context, computing the collapse loads for one million samples required only 3 to 4 min. The LAS method was employed to generate the large number of samples required due to its computational efficiency.

2.6 Calculation of the Probability of Failure

To estimate the probability of failure of the foundation, the performance function used was the factor of safety FS, determined for each sample, defined as the quotient between the true ultimate load supported by the footing, F_u, estimated from the RFELA computations for each sample, and the force to which the foundation can be subjected according to the design, F_{act}:

$$FS = \frac{F_u}{F_{act}} \tag{15}$$

The acting force F_{act} is considered non-deterministic, meaning that the applied force has a particular distribution based on $G_{MFA}^{\max}$ (Eq. (12)). The permanent load is assumed to follow a normal distribution, and the variable load a Gumbel distribution. The acting force can therefore be calculated as:

$$F_{act} = \mathrm{N}(G_{MFA}^{\max};0.1G_{MFA}^{\max}) + \mathrm{Gumbel}(XG_{MFA}^{\max};0.35XG_{MFA}^{\max}) \tag{16}$$

where the values 0.1 and 0.35 correspond to the coefficients of variation assumed in this work for the permanent and variable loads, respectively, obtained from the literature (Bartlett et al. 2003; Teixeira et al. 2011). In this equation, $\mathrm{N}(\mu;\sigma)$ denotes a realization of a normally distributed random variable with mean μ and standard deviation σ, while $\mathrm{Gumbel}(\mu;\sigma)$ denotes a realization of a Gumbel-distributed random variable with the given mean and standard deviation.

Once the FS values are determined for all samples, the probability of failure (P_f) is defined as the probability of the factor of safety being less than or equal to one:

$$P_f = P(FS \leq 1). \tag{17}$$

This probability is estimated in two ways. First, by dividing the number of samples in which $FS \leq 1$ by the total number of samples. Second, a lognormal distribution is fitted to the values of FS, and the probability of failure is calculated from this distribution. The choice of the lognormal distribution is justified because it provides the best fit among the normal, lognormal, gamma, Weibull, and exponential distributions, measured by the Root Mean Square Error parameter.

3 Overview of the Simulation Program

In summary, as previously described, the calculations are performed for: $B = 3\,\mathrm{m}$; $\mu_{s_u} = 100\,\mathrm{kPa}$; COV_{s_u} ranging from 0.1 to 0.5; $\theta_v = 1\,\mathrm{m}$ and 6 m; $\theta_h = 45\,\mathrm{m}$; and $\Gamma^2 = 0$, 1, and 0.48.

Two distinct approaches for determining the characteristic values of s_u are considered (Sect. 2.3): one based on the mean and coefficient of variation used to generate the samples (Table 1), and the other based on the mean and coefficient of variation obtained from the characterization simulation on each sample.

As described in Sect. 2.6, two methods for estimating the probability of failure are applied: a direct method and a method based on fitting a statistical distribution.

Additionally, the cases are analyzed for two sets of partial factors, representing the two relevant combinations prescribed by Eurocode 7, namely:

- Set 1: $\gamma_G = 1.0$; $\gamma_Q = 1.3$; $\gamma_{s_u} = 1.4$;
- Set 2: $\gamma_G = 1.35$; $\gamma_Q = 1.5$; $\gamma_{s_u} = 1.4$.

For each of the analysis cases defined above, the computations were carried out for different values of the load ratio $Q/(G+Q)$. This ratio represents the proportion of the variable load relative to the total applied load (permanent plus variable) and ranges from 0 to 0.9 in increments of 0.05, with the additional case 0.99 also included. A direct relationship can be defined between the load ratio and the scalar parameter X, specifically:

$$X = \frac{Q/(G+Q)}{1 - Q/(G+Q)} \tag{18}$$

4 Illustrative Example

This initial example corresponds to the following case:

- $COV_{s_u} = 0.3$; $\theta_v = 6\,\mathrm{m}$; $\Gamma^2 = 0$;

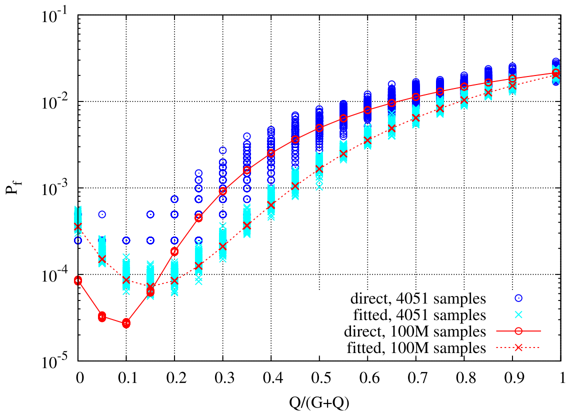

Fig. 4 Example of the calculations of the probability of failure for $COV_{s_u} = 0.3$; $\theta_v = 6\,\mathrm{m}$; $\Gamma^2 = 0$, s_{uk} determined from the mean and the coefficient of variation obtained from the simulation of characterization on each sample and for the set 1 of partial factors

- s_{uk} determined from the mean and the coefficient of variation obtained from the simulation of characterization on each sample;
- Set 1 of partial factors is used.

Results for this case, obtained from the initial 4051 samples and from the 100 million samples are presented in Fig. 4 as a function of $Q/(G+Q)$. These results were obtained from 100 simulations of the acting force, F_{act}, as given by Eq. (16). Probabilities of failure are shown for both direct calculations and for the fitted lognormal distribution.

Figure 4 shows that the 100 sets of simulations of F_{act} produce similar results for 100 M samples, but results in much greater variation for 4051 samples. With a very large number of samples, the FS distribution is essentially stable, whereas this is clearly not the case for 4051 samples.

It can also be seen that the fitted distribution for 4051 samples cannot reproduce the results of the probability of failure obtained directly from these samples. In addition, even the fitted distribution for 100 M samples does not match the direct results. Indeed, it closely follows the average of the fitted distribution for 4051 samples, under-predicting the probability of failure for some values of $Q/(G+Q)$ and over-predicting it for others.

Finally, the direct results from 4051 samples do not match those from 100 M samples, particularly for the lower values of $Q/(G+Q)$.

It can therefore be concluded that, of the four approaches shown in Fig. 4, only the direct results from 100 M samples can provide reliable conclusions. In the following section, the analyses are presented for this approach only.

It should be noted that sample sizes of 1 M and 10 M realizations were also tested. Although often adequate, these sizes did not consistently ensure stable results across all cases. Consequently, 100 M samples were adopted throughout. It is worth emphasizing again that the RFELA framework employed is fully capable of handling samples of this magnitude with very high computational efficiency.

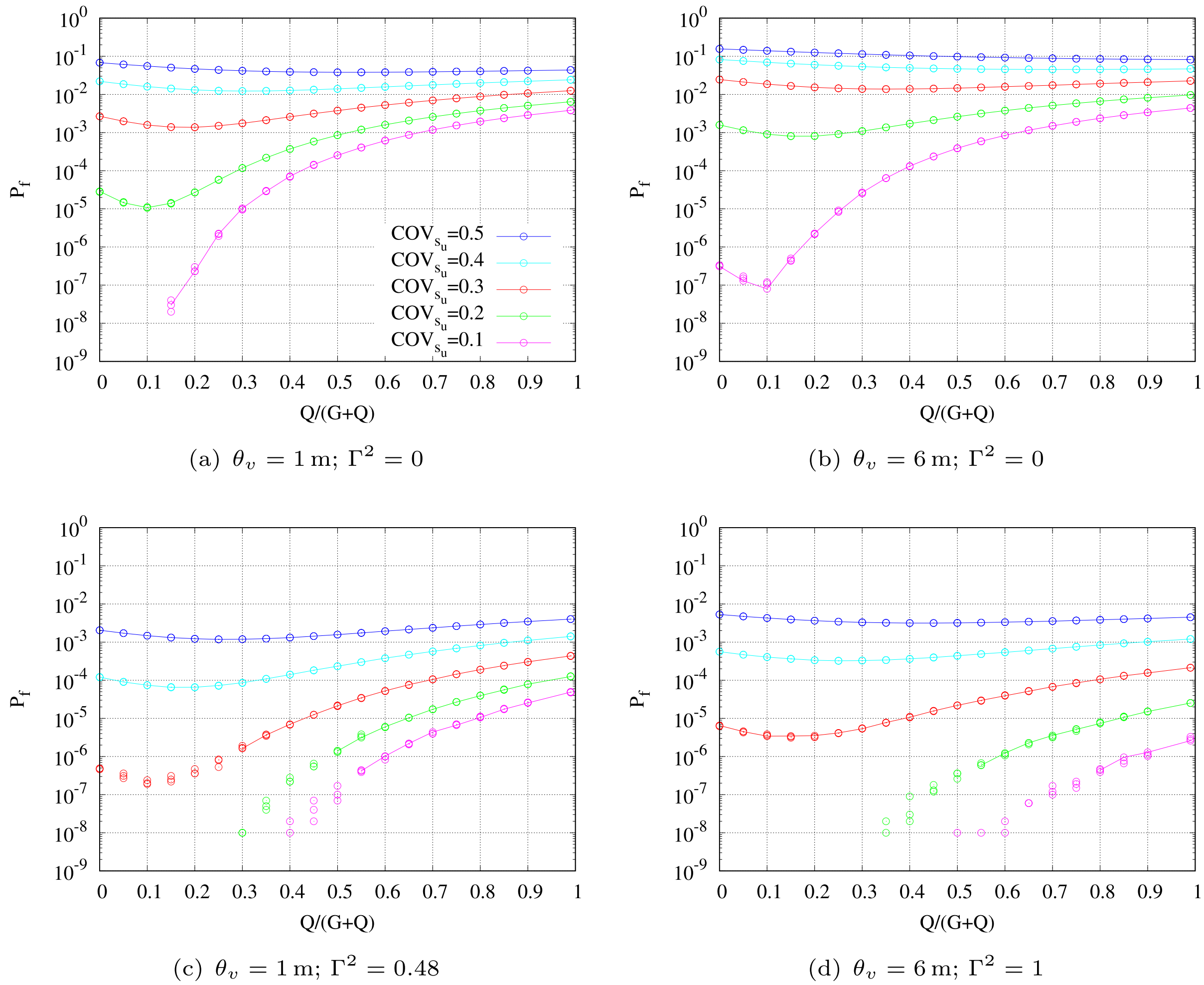

(a) $\theta_v = 1\,\mathrm{m}$; $\Gamma^2 = 0$ (b) $\theta_v = 6\,\mathrm{m}$; $\Gamma^2 = 0$

(c) $\theta_v = 1\,\mathrm{m}$; $\Gamma^2 = 0.48$ (d) $\theta_v = 6\,\mathrm{m}$; $\Gamma^2 = 1$

Fig. 5 Probabilities of failure obtained for the first set of partial factors and for the characteristic value of s_u based on the mean and COV_{s_u} used to generate the samples

5 Results

5.1 Set 1 of Partial Factors

The results presented in Fig. 5 were obtained for the first set of partial factors (where $\gamma_G = 1.0$, $\gamma_Q = 1.3$ and $\gamma_{s_u} = 1.4$) and for the characteristic value of s_u based on the mean and coefficient of variation of the undrained shear strength used to generate the samples, as shown in Table 1. For this figure and for the following figures of the same type, three calculations are shown considering the variation of the acting force (Eq. (16)) instead of the 100 that were shown in Fig. 4. In most cases presented, in particular for the most relevant ones (higher probability of failure), the three results are indistinguishable; however, when the probability of failure becomes very small (on the order of 10^{-7} or lower) this is no longer the case, showing a lower accuracy.

The analysis of Fig. 5 shows that the value of COV_{s_u} influences the probability of failure in all cases. A larger value of COV_{s_u} leads to greater probabilities of failure. For small values of $Q/(G+Q)$ the differences are of several orders of magnitude. For $\Gamma^2 = 0$, the probabilities of failure for the most relevant cases ($COV_{s_u} \geq 0.3$) are greater than 10^{-4}. For $\Gamma^2 = 0.48$ or 1 the probability of failure is still high, although not as high as for $\Gamma^2 = 0$. For the large values of COV_{s_u} the probability of failure is fairly independent of $Q/(G+Q)$; for the lower values of COV_{s_u}, the

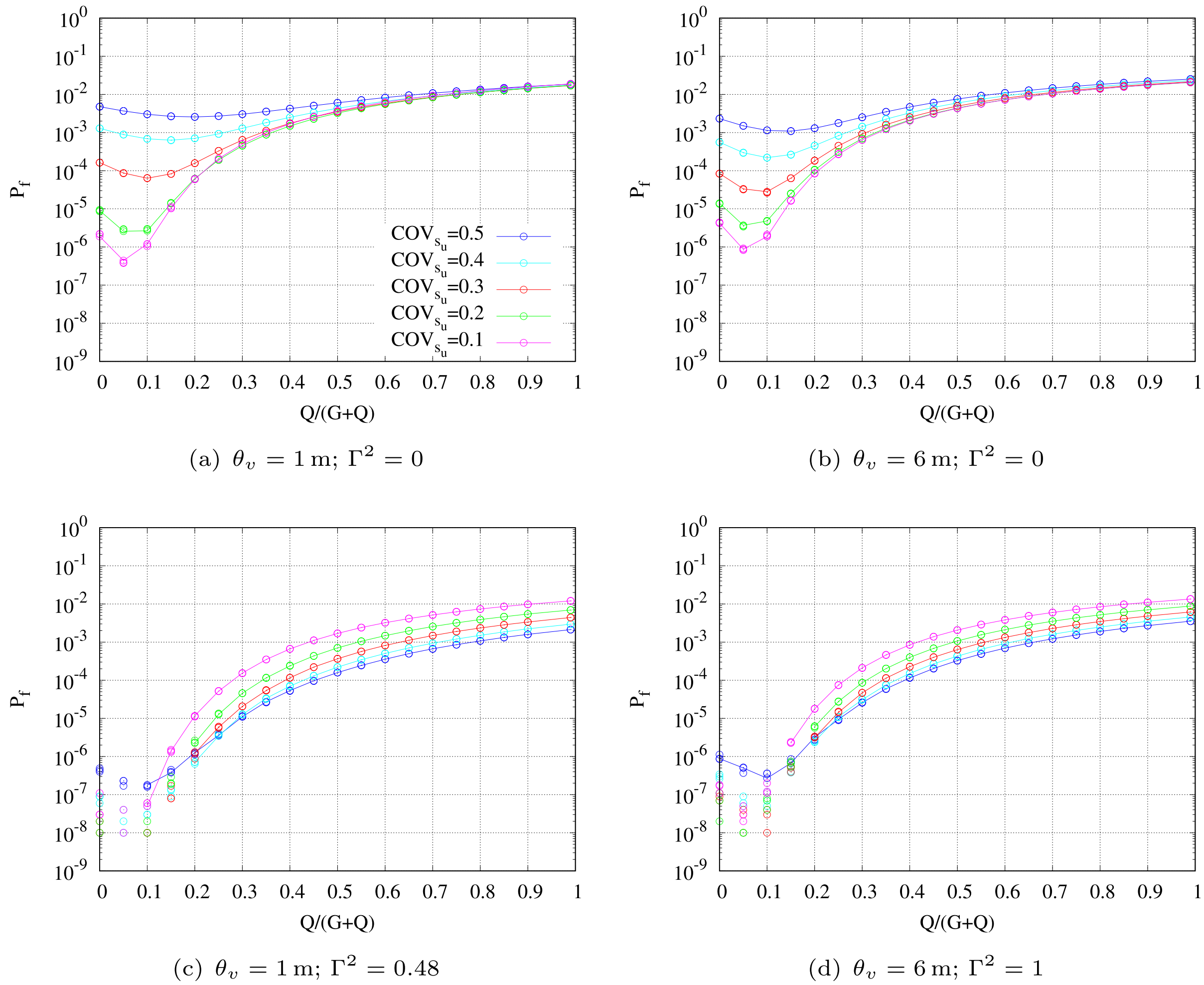

Fig. 6 Probabilities of failure obtained for the first set of partial factors and for the characteristic value of s_u determined from the mean and COV_{s_u} obtained from the simulation of characterization on each sample

probability of failure increases with $Q/(G+Q)$ except for the lower values of this parameter.

Figure 6 shows the results obtained for the same set of partial factors but with s_{uk} determined from the average and COV_{s_u} obtained from the simulation of characterization on each sample. For $\Gamma^2 = 0$ the value of COV_{s_u} influences the probability of failure but only for low to medium values of $Q/(G+Q)$. For these cases the probabilities of failure are high for the greater values of COV_{s_u}. For the greater values of $Q/(G+Q)$, the probability of failure becomes independent of COV_{s_u} and large in all cases.

For $\Gamma = 0.48$ or 1 the probability of failure is globally less dependent on COV_{s_u}, but this dependency exists even from values of $Q/(G+Q)$ greater than around 0.2. In this range the probability of failure is higher for the lower values of COV_{s_u} and it reaches quite high values for the larger $Q/(G+Q)$.

When comparing the results from Fig. 7 with those from Fig. 6, it can be seen that the probabilities of failure are lower for the latter, which means that, as could be expected, local soil characterization leads to a safer design.

5.2 Set 2 of Partial Factors

The results presented in Fig. 7 were obtained for the second set of partial factors (where $\gamma_G = 1.35$, $\gamma_Q = 1.5$ and $\gamma_{s_u} = 1.4$) and for the characteristic

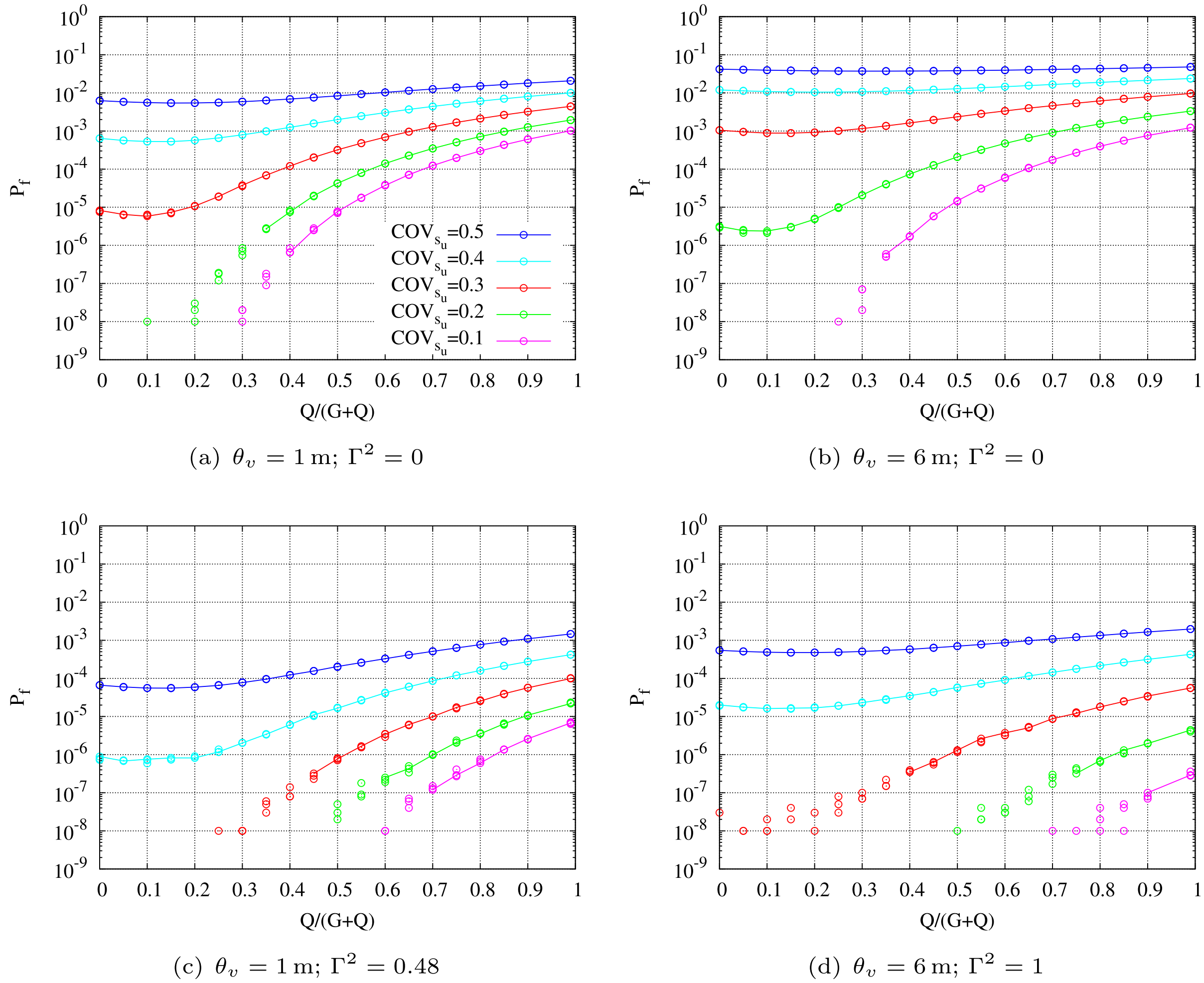

(a) $\theta_v = 1\,\mathrm{m};\ \Gamma^2 = 0$

(b) $\theta_v = 6\,\mathrm{m};\ \Gamma^2 = 0$

(c) $\theta_v = 1\,\mathrm{m};\ \Gamma^2 = 0.48$

(d) $\theta_v = 6\,\mathrm{m};\ \Gamma^2 = 1$

Fig. 7 Probabilities of failure obtained for the second set of partial factors and for the characteristic value of s_u based on the mean and COV_{s_u} used to generate the samples

value of s_u based on the mean and COV_{s_u} used to generate the samples. Figure 8 shows the results obtained for the same set of partial factors but with s_{uk} determined from the mean and COV_{s_u} obtained from the simulation of characterization on each sample.

The analyses of these figures show that the curves follow similar trend to those from Figs. 5 and 6, with lower probabilities of failure. This reduction was expected as the second set of partial factors are globally higher. However, there are still many situations in which the probability of failure is higher than 10^{-4}.

5.3 Comments

From this analysis, it can be said that considering the characteristic value of s_u based on the average and coefficient of variation used to generate the samples, which would be equivalent to not conducting any local characterization and relying on a good prior knowledge of the soil, is not adequate. Conducting local characterization is, as expected, very important to perform appropriate design. The following is therefore based on the results where such characterization was performed.

When using the first set of partial factors, estimates of the characteristic value based on the average ($\Gamma^2 = 0$) lead to probabilities of failure that are very

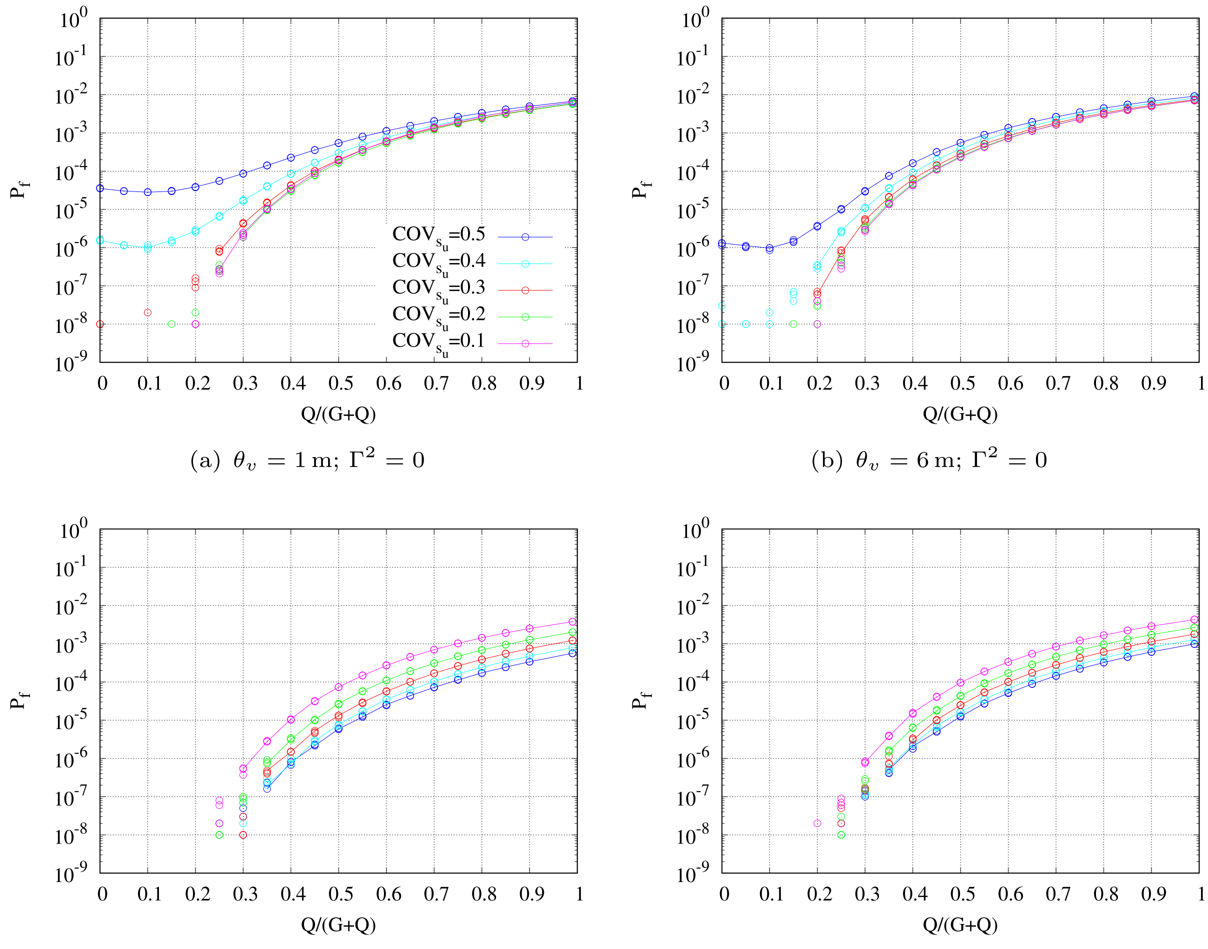

(a) $\theta_v = 1\,\mathrm{m}$; $\Gamma^2 = 0$

(b) $\theta_v = 6\,\mathrm{m}$; $\Gamma^2 = 0$

(c) $\theta_v = 1\,\mathrm{m}$; $\Gamma^2 = 0.48$

(d) $\theta_v = 6\,\mathrm{m}$; $\Gamma^2 = 1$

Fig. 8 Probabilities of failure obtained for the second set of partial factors and for the characteristic value of s_u determined from the mean and COV_{s_u} obtained from the simulation of characterization on each sample

dependent on the coefficient of variation for the lower values of $Q/(G+Q)$ and, for most situations analyzed, it is greater than 10^{-4}. Estimates based on the appropriate sensitivity index ($\Gamma^2 = 0.48$ or 1) result in low probabilities of failure for $Q/(G+Q)$ less than 0.25. For these cases, it is interesting to notice that the higher probabilities of failure are obtained for the lower coefficients of variation. In an ideal design method, the probability of failure would be independent of the value of the coefficient of variation, as this coefficient would have been adequately considered when determining the characteristic value of the soil strength.

When using the second set of partial factors, it seems possible to use the estimates of the characteristic values based on the average ($\Gamma^2 = 0$) and on the more appropriate sensitivity index ($\Gamma^2 = 0.48$ or 1). For the first case, however, the probability of failure is, again, very dependent on the coefficient of variation for the lower values of $Q/(G+Q)$. Those probabilities are lower than 10^{-4} for $Q/(G+Q) < 0.3$. For the second case ($\Gamma^2 = 0.48$ or 1) the probabilities of failure are lower than 10^{-4} for $Q/(G+Q)$ less than 0.5, for $COV_{s_u} = 0.1$, and for $Q/(G+Q)$ less than 0.65, for $COV_{s_u} = 0.3$.

All results seem to indicate that, for the greater values of $Q/(G+Q)$, the variable action should be affected by a greater partial factor. On the other

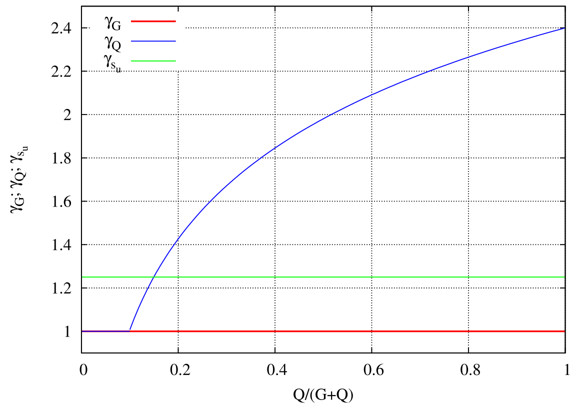

Fig. 9 Proposed partial coefficients (see Eqs. 19–22) for characteristic values of s_u determined using appropriate values of Γ^2

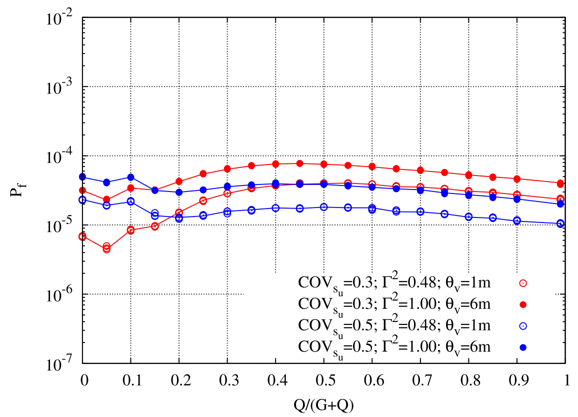

Fig. 10 Probabilities of failure resulting from the proposed set of partial factors (see Eqs. 19–22 and Fig. 9) and for s_{uk} determined from the average and from the coefficient of variation obtained from the simulation of characterization on each sample

hand, for $\Gamma^2 = 0.48$ or 1, the obtained probabilities of failure for the lower values of $Q/(G+Q)$ are very low. This leads to the possibility of defining a new set of partial factors that, for this case ($\Gamma^2 = 0.48$ or 1), would result in probabilities of failure less dependent on $Q/(G+Q)$. Towards this objective the authors concluded that the coefficient γ_Q would have to be dependent on $Q/(G+Q)$. The following set is therefore proposed (see also Fig. 9):

$$\gamma_G = 1.0 \tag{19}$$

$$\gamma_Q = 1.0 \text{ for } Q/(G+Q) \le 0.1 \tag{20}$$

$$\gamma_Q = 0.605 \ln[Q/(G+Q)] + 2.4 \text{ for } Q/(G+Q) > 0.1 \tag{21}$$

$$\gamma_{s_u} = 1.25 \tag{22}$$

This set, combined with local characterization and appropriate values of Γ^2, leads to reasonable probabilities of failure for coefficients of variation of 0.3 to 0.5, as this range is the most relevant for the undrained shear strength (Schneider et al. 2013). Figure 10 shows those probabilities of failure.

6 Concluding Remarks

A simple problem of the bearing capacity of a shallow foundation subjected to centered and vertical loading, supported by soil responding under undrained conditions, was studied. For this problem, the probabilities of failure were determined, considering the variability of the undrained shear strength and its spatial distribution, different levels of knowledge of the soil properties, and different sets of partial factors.

It was shown that the probabilities of failure are not adequately predicted when using a relatively small number of samples combined with fitting a statistical distribution function to the results of those samples. The calculations were therefore performed using a methodology that allows a large number of samples without the need for any fitting.

The initial sets of partial factors cannot ensure a relatively constant probability of failure for a wide range of $Q/(G+Q)$. In some cases, they are greater than 10^{-4}, and in other cases, they reach very low values. To address these issues, a proposal for a new set of partial factors was made. Although this set of partial factors is derived from the simple case of a foundation resting on the soil surface, in the authors' opinion it should be expected that in the case of a small depth of the foundation, the relatively small contribution to the bearing capacity of soil above its base under undrained conditions would not affect the results in a significant way, particularly if the strength of the soil above the foundation base is to be neglected in the analysis.

It was also shown that local characterization, combined with the use of the sensitivity index, results in a characteristic value of the undrained shear strength that leads to an adequate design.

Author Contributions All authors contributed equally to tis paper

Funding Open access funding provided by FCT|FCCN (b-on). This work was partially supported by the Foundation for Science and Technology (FCT) through the project UIDB/04,625/2025 of the research unit CERIS.

Data Availability All data, models, and specific code routines that support the findings of this study are available from the corresponding author upon reasonable request.

Declarations

Conflict of Interest The authors declare they have no conflict of interest.

References

Alonso EE (1976) Risk analysis of slopes and its application to slopes in Canadian sensitive clays. Géotechnique 26(3):453–472. https://doi.org/10.1680/geot.1976.26.3.453

Antão A, da Silva MV, Guerra N et al (2012) An upper bound-based solution for the shape factors of bearing capacity of footings under drained conditions using a parallelized mixed f.e. formulation with quadratic velocity fields. Comput Geotech 41:23–35. https://doi.org/10.1016/j.compgeo.2011.11.003

Antão A, Guerra N, Vicente da Silva M, et al (2019) Upper and lower bounds for the bearing capacity of foundations on soft soils with reinforcement columns. In: Proceedings of the 17th European conference on soil mechanics and geotechnical engineering

Antão A, Vicente da Silva M, Monteiro N et al (2021) Upper and lower bounds for three-dimensional undrained stability of shallow tunnels. Transportation Geotechnics 27:100491. https://doi.org/10.1016/j.trgeo.2020.100491

Bartlett FM, Hong HP, Zhou W (2003) Load factor calibration for the proposed 2005 edition of the national building code of canada: companion-action load combinations. Can J Civ Eng 30(2):440–448. https://doi.org/10.1139/l02-086

Chen XJ, Fu Y, Liu Y (2022) Random finite element analysis on uplift bearing capacity and failure mechanisms of square plate anchors in spatially variable clay. Eng Geol 304:106677. https://doi.org/10.1016/j.enggeo.2022.106677

Cheng P, Liu Y, Li YP et al (2022) A large deformation finite element analysis of uplift behaviour for helical anchor in spatially variable clay. Comput Geotech 141:104542. https://doi.org/10.1016/j.compgeo.2021.104542

Cheng P, Guo J, Yao K et al (2023) Numerical investigation on pullout capacity of helical piles under combined loading in spatially random clay. Mar Geores Geotechnol 41(10):1118–1131. https://doi.org/10.1080/1064119X.2022.2120843

Cheng P, Hu Y, Yao K et al (2023) Probabilistic investigations on the elastic stiffness coefficients for suction caisson considering spatially varying soils. Ocean Eng 289:116273. https://doi.org/10.1016/j.oceaneng.2023.116273

Cheng P, Liu F, Chen X et al (2024) Estimation of the installation torque—capacity correlation of helical pile considering spatially variable clays. Can Geotech J 61(10):2064–2074. https://doi.org/10.1139/cgj-2023-0331

Chwała M (2020) On determining the undrained bearing capacity coefficients of variation for foundations embedded on spatially variable soil. Studia Geotechnica et Mechanica 42(2):125–136. https://doi.org/10.2478/sgem-2019-0037

EN 1997–1 (2004) Eurocode 7, geotechnical design, Part 1: General rules. CEN, European Committee for Standardization, Brussels

Fan S, Zhang Y, Li S (2024) Fully assessing foundation failure envelopes under combined loads in spatially variable clay. Acta Geotech 19(5):3039–3057. https://doi.org/10.1007/s11440-023-02214-7

Fan S, Zhang Y, Li S et al (2025) A machine learning based framework for the probability failure envelope analysis of foundations in spatially variable clay. Eng Appl Artif Intell 143:110005. https://doi.org/10.1016/j.engappai.2025.110005

Fenton G, Griffiths D (2008) Risk Assessment in Geotechnical Engineering. John Wiley & Sons, New Jersey

Fenton G, Griffiths D (2025) The random finite element method (RFEM). http://random.engmath.dal.ca/rfem/, available 20 Dec

Griffiths D, Fenton GA (2001) Bearing capacity of spatially random soil: the undrained clay Prandtl problem revisited. Géotechnique 51(4):351–359. https://doi.org/10.1680/geot.2001.51.4.351

Griffiths DV, Zhu D, Fenton GA (2025) Importance of spatial variability in probabilistic stability analysis of relatively steep undrained slopes with a foundation layer. Int J Numer Anal Meth Geomech. https://doi.org/10.1002/nag.70087

Huang J, Griffiths D (2015) Determining an appropriate finite element size for modelling the strength of undrained random soils. Comput Geotech 69:506–513. https://doi.org/10.1016/j.compgeo.2015.06.020

Kounlavong K, Shiau J, Sangjinda K et al (2025) Stochastic analysis of safety factors for buried box pipelines in spatially random clay. Geotech Geol Eng 43(2):120. https://doi.org/10.1007/s10706-025-03083-5

Li Y, Chen X, He P et al (2025) Probabilistic analysis of slopes designed by the partial material factor approach. Comput Geotech 188:107572. https://doi.org/10.1016/j.compgeo.2025.107572

Liu H, Chen X, Cheng P et al (2025) An efficient approach for determination of equivalent design strength and probability of failure for tunnel face in spatially random soils. Structures 73:108346. https://doi.org/10.1016/j.istruc.2025.108346

Lumb P (1966) The variability of natural soils. Can Geotech J 3(2):74–97. https://doi.org/10.1139/t66-009

NP122 (2010) Standard on the determination of characteristic values and design values of geotechnical parameters. Romanian Technical Norm. (in Romanian)

Olsson A, Sandberg G, Dahlblom O (2003) On Latin hypercube sampling for structural reliability analysis. Struct Saf 25(1):47–68. https://doi.org/10.1016/S0167-4730(02)00039-5

Orr T, Sorgatz J, Estaire J, et al (2025) Determination of representative values from derived values for verification with limit states with EN 1997. Tech. rep., Publications Office of the European Union, Luxembourg, https://doi.org/10.2760/0980105

Paice GM, Griffiths DV, Fenton GA (1996) Finite element modeling of settlements on spatially random soil. J Geotec Eng 122(9):777–779. https://doi.org/10.1061/(ASCE)0733-9410(1996)122:9(777)

Phoon KK, Kulhawy FH (1999) Characterization of geotechnical variability. Can Geotech J 36(4):612–624. https://doi.org/10.1139/t99-038

Puła W, Griffiths D (2021) Transformations of spatial correlation lengths in random fields. Comput Geotech 136:104151. https://doi.org/10.1016/j.compgeo.2021.104151

Rogério F, Guerra N, Antão A et al (2024) Soil strength parameters for the sustainable design of unsupported cuts under drained conditions using reliability analysis. Sustainability 16(23):10596. https://doi.org/10.3390/su162310596

Santana T, Vicente da Silva M, Antão A et al (2018) Two dimensional upper and lower-bound numerical analysis of the basal stability of deep excavations in clay. In: Cardoso AS, Borges JL, Costa PA et al (eds) Numerical Methods in Geotechnical Engineering IX, Sociedade Portuguesa de Geotecnia and FEUP. Taylor and Francis, Porto, pp 1197–1202

Schneider HR, Schneider MA (2013) Dealing with uncertainties in EC7 with emphasis on determination of characteristic soil properties. In: Arnold P, Fenton GA, Hicks MA et al (eds) Modern geotechnical design codes of practice. Implementation, application and development, advances in soil mechanics and geotechnical engineering

Siacara AT, Beck AT, Ji J (2024) Impact of random field simulations on fem-based earth slope reliability. Geotech Geol Eng 42(8):7873–7891. https://doi.org/10.1007/s10706-024-02956-5

Vicente da Silva M, Antão AN (2025) Finite-element limit analysis formulation using Bishop's strength criterion for anisotropic undrained soils. Int J Geomech 25(4):04025037. https://doi.org/10.1061/IJGNAI.GMENG-10432

Vicente da Silva M, Antão AN (2025) A new random field finite-element limit analysis approach for undrained soils. Géotec Lett 16:1–6. https://doi.org/10.1680/jgele.25.00023

Simões J, Neves LC, Antão AN et al (2020) Reliability assessment of shallow foundations on undrained soils considering soil spatial variability. Comput Geotech 119:103369. https://doi.org/10.1016/j.compgeo.2019.103369

Simões JT, Neves LC, Antão AN et al (2014) Probabilistic analysis of bearing capacity of shallow foundations using three-dimensional limit analyses. Int J Comput Methods 11(02):1342008. https://doi.org/10.1142/S0219876213420085

Teixeira A, Correia A, Honjo Y, et al (2011) Reliability analysis of a pile foundation in a residual soil: contribution of the uncertainties involved and partial factors. In: Vogt, Schuppener, Straub, et al (eds) 3rd international symposium on geotechnical safety and risk (ISGSR2011)

Vanmarcke E (1980) Probabilistic stability analysis of earth slopes. Eng Geol 16(1):29–50. https://doi.org/10.1016/0013-7952(80)90005-8

Vanmarcke EH (1977) Probabilistic modeling of soil profiles. J Geotech Eng Div 103(11):1227–1246. https://doi.org/10.1061/AJGEB6.0000517

Viana L, Antão A, Vicente da Silva M, et al (2019) The application of limit analysis to the study of the basal failure of deep excavations in clay considering the spatial distribution of soil strength. In: Proceedings of the 17th European conference on soil mechanics and geotechnical engineering

Vicente da Silva M, Deusdado N, Antão A (2020) Lower and upper bound limit analysis via the alternating direction method of multipliers. Comput Geotech 124:103571. https://doi.org/10.1016/j.compgeo.2020.103571